Since January 2020 Elsevier has created a COVID-19 resource centre with free information in English and Mandarin on the novel coronavirus COVID-19. The COVID-19 resource centre is hosted on Elsevier Connect, the company's public news and information website.

Antiviral Research 111 (2014) 78–81

Contents lists available at ScienceDirect

Antiviral Research

journal homepage: www.elsevier.com/locate/antiviral

Short Communication

Crystal structure of dengue virus methyltransferase without *S*-adenosyl-*L*-methionine

Christian G. Noble, Shi-Hua Li, Hongping Dong, Sock Hui Chew, Pei-Yong Shi *

Novartis Institute for Tropical Diseases, 10 Biopolis Road, 05-01 Chromos, Singapore 138670, Singapore

ARTICLE INFO

Article history:
Received 25 July 2014
Revised 3 September 2014
Accepted 9 September 2014
Available online 19 September 2014

Keywords:
Flavivirus
Dengue virus
Enzyme
Crystal structure
Structure-based design
Methyltransferase

ABSTRACT

Flavivirus methyltransferase is a genetically-validated antiviral target. Crystal structures of almost all available flavivirus methyltransferases contain *S*-adenosyl-*L*-methionine (SAM), the methyl donor molecule that co-purifies with the enzymes. This raises a possibility that SAM is an integral structural component required for the folding of dengue virus (DENV) methyltransferase. Here we exclude this possibility by solving the crystal structure of DENV methyltransferase without SAM. The SAM ligand was removed from the enzyme through a urea-mediated denaturation-and-renaturation protocol. The crystal structure of the SAM-depleted enzyme exhibits a vacant SAM-binding pocket, with a conformation identical to that of the SAM-enzyme co-crystal structure. Functionally, equivalent enzymatic activities (N-7 methylation, 2′-*O* methylation, and GMP-enzyme complex formation) were detected for the SAM-depleted and SAM-containing recombinant proteins. These results clearly indicate that the SAM molecule is not an essential component for the correct folding of DENV methyltransferase. Furthermore, the results imply a potential antiviral approach to search for inhibitors that can bind to the SAM-binding pocket and compete against SAM binding. To demonstrate this potential, we have soaked crystals of DENV methyltransferase without a bound SAM with the natural product Sinefungin and show that preformed crystals are capable of binding ligands in this pocket.

Eukaryotic cellular mRNA and most viral RNAs share a common 5′ type-1 cap structure (m7GpppNm). The cap structure is essential for RNA splicing, transport, stability, and translation (Ghosh and Lima, 2010). Four enzymatic reactions are required for the type-1 cap formation: (i) an RNA triphosphatase removes the γ-phosphate from the 5′ triphosphate of the nascent RNA (pppN-RNA → ppN-RNA); (ii) an RNA guanylyltransferase (GTase) transfers the GMP moiety from GTP to ppN-RNA to generate GpppN-RNA (GTP + ppN-RNA → GpppN-RNA); (iii) an N-7 methyltransferase (MTase) methylates the guanine N-7 position to produce m7GpppN-RNA (GpppN-RNA → m7GpppN); (iv) a 2′-*O* MTase methylates the ribose 2′-*O* position of the RNA to complete the type-1 cap formation (m7GpppN-RNA → m7GpppNm). Both N-7 and 2′-*O* methylations use *S*-adenosyl-*L*-methionine (SAM) as a methyl donor and generate *S*-adenosyl-*L*-homocysteine (SAH) as a by-product (Decroly et al., 2012).

The SAM molecule always co-purifies with dengue virus (DENV) MTase. This is also true for almost all known flavivirus MTases (Assenberg et al., 2007; Bollati et al., 2009; Egloff et al., 2002; Geiss et al., 2009; Jansson et al., 2009; Mastrangelo et al., 2007; Zhou et al., 2007). The only known exception is the Modoc virus MTase (Jansson et al., 2009). For the DENV MTase, we have performed extensive dialysis to remove the bound SAM, but the ligand always remained bound to the MTase (unpublished data). This observation raises the question of whether the SAM molecule is an integral structural component required for the folding of DENV and closely related flavivirus MTases (Noble and Shi, 2012). To address this question, we investigated the structural and enzymatic integrity of DENV MTase in the absence of SAM.

DENV belongs to the *Flavivirus* genus within the Flaviviridae family. It contains a single-strand, plus-sense RNA with a 5′ type-1 cap. The N-terminal third of the flavivirus nonstructural protein 5 (NS5) encodes N-7 MTase (Ray et al., 2006), 2′-*O* MTase (Egloff et al., 2002), internal RNA MTase (Dong et al., 2012), and GTase (Bollati et al., 2009; Egloff et al., 2007; Issur et al., 2009). Here we report that structurally and functionally integrated recombinant DENV-3 MTase without a SAM molecule can be obtained using a urea-mediated denaturation-and-renaturation process. The crystal structure of the SAM-depleted MTase is identical to that of the SAM-MTase complex. The SAM-depleted and SAM-containing MTases exhibited comparable enzymatic activities (N-7 MTase, 2′-*O* MTase, and covalent GMP-MTase complex formation). Preformed crystals of the refolded DENV MTase were soaked with

* Corresponding author. Tel.: +65 67222909; fax: +65 67222916.
E-mail address: pei_yong.shi@novartis.com (P.-Y. Shi).

http://dx.doi.org/10.1016/j.antiviral.2014.09.003
0166-3542/

the natural product Sinefungin, showing that this is a viable approach to identify novel small molecules that bind to the same pocket.

Preparation of SAM-depleted recombinant MTase: We used a urea-mediated denaturation-and-renaturation procedure to remove the SAM molecule that co-purified with the DENV-3 MTase. The expression and purification protocol was reported previously (Lim et al., 2011). Briefly, the MTase domain representing the 262 amino acids of DENV-3 NS5 was fused with an N-terminal glutathione-*S*-transferase and purified by glutathione affinity. The tag was removed by cleavage with Prescission protease. To remove the co-purified SAM, we denatured the purified protein in 20 mM HEPES, pH 7.0, 300 mM NaCl, and 2 mM DTT by addition of 8 M urea and exhaustively dialyzed the protein against a buffer containing 8 M urea, 20 mM HEPES, pH 7.0, 300 mM NaCl, and 2 mM DTT. The MTase was refolded by concentrating the protein, followed by 8-times rapid dilution into the same buffer lacking urea, to give a final concentration of 1 M urea. The refolded MTase was further purified by size-exclusion chromatography. As shown in Fig. 1A, the SAM-containing MTase and SAM-depleted MTase migrated at equivalent positions on a 12% SDS–PAGE gel. The absence of SAM was demonstrated by precipitating the protein with perchloric acid and removing the precipitant by centrifugation as described previously (Noble et al., 2007). The supernatant containing the solubilized nucleotide was then analyzed by measuring the absorbance at 260 nm. The native recombinant MTase protein treated this way showed a typical adenosine absorbance spectrum, whilst the refolded MTase, showed no absorbance (data not shown). The lack of a bound SAM was confirmed by determining the crystal structure of the SAM-depleted protein (see below).

Enzymatic activities of SAM-depleted MTase: To examine the effect of SAM depletion on the function of MTase, we compared three enzymatic activities between the wild-type (WT) MTase with co-purified SAM and the refolded MTase depleted of SAM. We first analyzed cap-methylation activities in the presence of additional 50 μM SAM. Equivalent N-7 methylation (Fig. 1B) and 2′-*O* methylation (Fig. 1C) were detected for both the SAM-containing and SAM-depleted MTases. The N-7 and 2′-*O* methylation assays were performed as previously described (Dong et al., 2010). Briefly, The ^{33}P-labeled G*pppA-RNA and m7G*pppA-RNA (The asterisk indicates that the following phosphate is labeled with ^{33}P) were used for N-7 and 2′-*O* methylations, respectively. The RNA substrate consisted of the first 211 nucleotides of the DENV-3 genome. The N-7 methylation was performed in a 20-μl reaction containing 50 mM Bis–Tris [pH 6.0], 50 mM NaCl, 2 mM dithiothreitol [DTT], ~3×10^5 cpm G*pppA-RNA, 50 μM SAM, and 1 μg MTase; the reaction was incubated at 22 °C for 5 min. The 2′-*O* methylation was performed in a 20-μl volume containing 50 mM Tris–HCl [pH 9.0], 1 mM $MgCl_2$, 2 mM DTT, ~3×10^5 cpm m7G*pppA-RNA, 50 μM SAM, and 1 μg MTase; the reaction was incubated at 22 °C for 1 h. Both N-7 and 2′-*O* reactions were stopped by phenol–chloroform extraction followed by ethanol precipitation. The methylated RNA products were re-suspended in RNase-free H_2O, digested with nuclease P1 (Sigma–Aldrich) overnight, and analyzed on polyethyleneimine cellulose thin-layer chromatography (TLC) plates (JT Baker) using an aqueous solution containing 0.65 M LiCl. The radioactive cap variants (G*pppA, m7G*pppA, and m7G*pppAm) on TLC plates were quantified by a PhosphorImager (Typhoon; GE Healthcare).

Next, we analyzed the formation of a covalent GMP-MTase complex. A GTase capping is mediated by a two-step ping-pong reaction: the GMP moiety from GTP is first covalently linked to the GTase to form a GMP-GTase complex; the GMP-GTase complex then transfers the GMP to the 5′-end of ppN-RNA to produce GpppN-RNA (Shuman and Hurwitz, 1981). For flavivirus, the GMP-MTase (functioning as a GTase) complex can be readily formed via a phosphoamide bond to an attacking Lys of the enzyme, whereas the conversion to the product GpppN-RNA is not efficient (Bollati et al., 2009; Issur et al., 2009). As shown in Fig. 1D, similar amounts of GMP-MTase complex were formed by the SAM-containing and SAM-depleted MTases. The GMP-MTase complex was formed in a 20-μl reaction containing 1 μg DENV-3 SAM-containing or SAM-depleted MTase, 50 mM Tris (pH 8.0), 6 mM KCl, 1.25 mM $MgCl_2$, 1.25 mM DTT, and 50 μCi α-^{33}P-GTP. After incubation at 37 °C for 1.5 h, the reaction was terminated by heating at 95 °C for 10 min and analyzed on a 12% SDS–PAGE

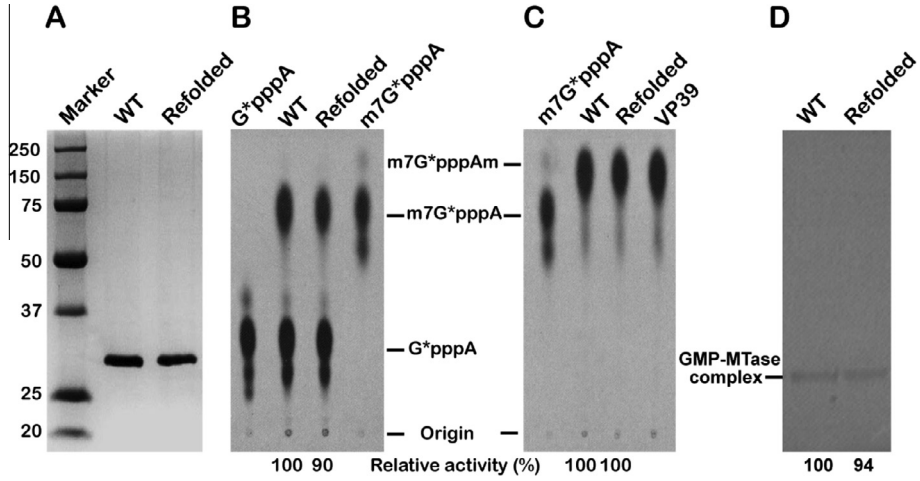

Fig. 1. Comparison of enzymatic activities of recombinant MTase proteins with or without bound SAM. (A) SDS–PAGE analysis of recombinant MTase with or without bound SAM. "Wild-type" (WT) MTase, representing the first 262 amino acids of NS5, contains bound SAM. "Refolded" MTase does not contain bound SAM. The molecular masses of protein markers are labeled on the left of the 12% SDS–PAGE. (B) N-7 methylation. The N-7 methylation activity was measured by the conversion of G*pppA-RNA to m7G*pppA-RNA in the presence of 50 μM SAM. Asterisks indicate the phosphate is labeled with ^{33}P. The methylation efficiency of the SAM-depleted MTase was compared with that of the SAM-containing MTase (set at 100%). Average results of three independent experiments are indicated at the bottom of the TLC image. The ^{33}P-labeled m7G*pppA and G*pppA markers are indicated on the top of the TLC plate. (C) 2′-*O* methylation. The 2′-*O* methylation activity was measured by conversion of m7G*pppA-RNA to m7G*pppAm-RNA in the presence of 50 μM SAM. The relative activity of 2′-*O* methylation in comparison with the WT activity (set at 100%) is shown below the TLC image. Average results of three independent experiments are shown. Vaccinia virus VP39, a well-characterized 2′-*O* MTase (Hodel et al., 1996), was included as a positive control. (D) Formation of covalently-linked GMP-enzyme complex. The reactions were performed with 1 μg of the WT or refolded MTase proteins in the presence of 50 μCi α-^{33}P-GTP (see text for details). The reactions were analyzed on a 12% SDS–PAGE. The gel was dried and analyzed using a PhosphorImager.

gel. After drying the gel, the α-^{33}P-GMP-MTase complex was visualized and quantified with a PhosphorImager. Taken together, the above results showed that depletion of SAM from the recombinant MTase does not significantly affect its N-7 MTase, 2′-*O* MTase, or GMP-MTase complex-formation activities.

Crystal structure of SAM-depleted MTase: To compare the conformation of the SAM-depleted MTase with the structure of the SAM-bound MTase, we determined the high resolution crystal structure of the refolded DENV-3 MTase to 1.46 Å resolution using the crystallization conditions described previously (Lim et al., 2011). Briefly, 1 μl of the protein at 10 mg/ml was mixed with 1 μL of a reservoir solution of 22.5% PEG 8000, 0.2 M NaCl, 0.1 M Tris–HCl, pH 8.5, and 20 mM tri-sodium citrate and crystallized by hanging-drop vapor diffusion. Crystals were transferred to the same solution supplemented with 10% glycerol for shock-cooling. The data were processed using the Global Phasing software suite (www.globalphasing.com) and the structure solved using PDB ID 3P97 as an initial model (Lim et al., 2011). The overall structure of the SAM-depleted MTase is very similar to the SAM-bound structure with a root mean square deviation (RMSD) of 0.170 Å for all Cα atoms (Table 1 and Fig. 2). A surface representation of the ligand-free MTase (Fig. 2A) shows that the DENV MTase in the absence of a ligand retains the large cavity for binding SAM. To determine whether this cavity of the enzyme is still capable of binding ligands, we soaked pre-formed crystals of the SAM-depleted MTase with the natural product Sinefungin and determined the structure. Crystals were soaked by adding 5 μl of the reservoir solution supplemented with 1 mM Sinefungin directly to the crystallization drop and equilibrating the crystals overnight. The structure of the complex shows that this enzyme is capable of binding the SAM analog Sinefungin in this pocket, without significant structural rearrangement; the RMSD for the free MTase and Sinefungin-bound structures is 0.223 Å for all Cα atoms, whilst between the SAM- and Sinefungin-bound structures it is 0.136 Å for all Cα atoms. A comparison of the three structures (bound to SAM, bound to Sinefungin, and ligand free) shows that there is no conformational change to the Cα backbone upon ligand binding

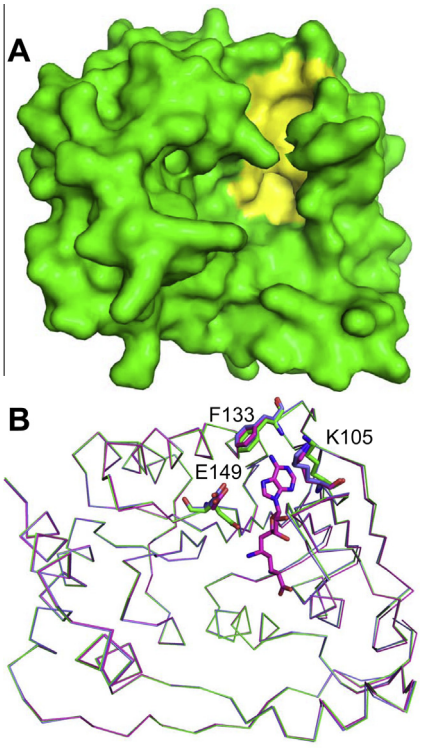

Fig. 2. Comparison of the crystal structures of DENV-3 MTase bound to SAM, Sinefungin or no ligand. (A) Surface representation of the SAM-depleted MTase, showing the intact cavity of the SAM binding site. Residues lining this cavity are colored yellow. (B) Ribbon representation of the Cα backbone of the free MTase (green), the SAM-bound MTase (3P97; purple), and the Sinefungin-bound MTase (pink). The bound Sinefungin molecule is shown as pink sticks and the residues discussed in the text are shown in sticks with the same coloring as the Cα ribbon. The images were generated using Pymol (www.pymol.org). (For interpretation of the references to color in this figure legend, the reader is referred to the web version of this article.)

Table 1
Data collection and refinement statistics. The values in parentheses refer to the highest resolution shell.

	MTase_Sinefungin	MTase_free
Wavelength (Å)	1.0	1.0
Resolution range (Å)	31.45–1.48 (1.56–1.48)	57.93–1.46 (1.60–1.46)
Space group	P 2 21 21	P 2 21 21
Cell parameters (*a*, *b*, *c*; Å)	51.64 61.14 183.35	52.08 61.09 182.35
Observed reflections	1,112,088 (165,363)	974,050 (230,053)
Unique reflections	97,039 (13,980)	97,696 (22,662)
Multiplicity	11.5 (11.8)	10.0 (10.2)
Completeness (%)	99.97 (99.85)	96.54 (94.45)
Mean *I*/sigma (I)	16.36 (4.19)	17.03 (2.58)
R-merge	0.073 (0.458)	0.074 (0.650)
R-factor	0.1964	0.2018
R-free	0.2145	0.2179
Number of atoms	5016	4913
Macromolecules	4170	4114
Ligands	54	–
Water	792	799
Protein residues	512	512
Average B factor		
Protein; waters; ligand	21.0; 36.1; 14.6	20.2; 34.4; –
RMS deviations (bonds; Å)	0.010	0.010
RMS deviations (angles; °)	1.03	1.03
Ramachandran plot		
Favored regions (%)	99.5	99.5
Disallowed regions (%)	0.5	0.5
PDB code	4R8S	4R8R

(Fig. 2B) and only modest movements of amino acid sidechains. The most obvious of these is a flip of Glu149, which is pointing towards the pocket in the free structure, but oriented away in the SAM- and Sinefungin-bound structures. Phe133 moves slightly towards the pocket in the free structure (~0.7 Å) and Lys105 moves slightly away (~1.5 Å). The structures of the complex show that the SAM-depleted MTase can be used for screening and structure-based design of novel inhibitors that bind to the SAM pocket. Taken together with the biochemical data, they strongly indicate that the presence of the ligand SAM is not required for the correct folding of DENV MTase.

Targeting the SAM-binding pocket as a potential antiviral approach: DENV represents the most prevalent mosquito-borne viral pathogen in humans. There is currently no clinically-approved vaccine or antiviral for DENV. Although great advances have been made toward to the development of DENV vaccines and drugs (Fink and Shi, 2014; Lim et al., 2013), new approaches are urgently needed to combat this global human pathogen. Recent studies showed that mutant viruses defective in 2′-*O* MTase are potential vaccine candidates for DENV (Zust et al., 2013), Japanese encephalitis virus (Li et al., 2013), and severe-acute respiratory-syndrome coronavirus (Menachery et al., 2014). Mutagenesis analysis revealed that defective N-7 MTase was lethal for flavivirus replication, suggesting that MTase is a potential antiviral target (Dong et al., 2014).

The current study demonstrates that SAM is not an essential structural element for the folding of DENV MTase. This conclusion was supported by two complementary structural and functional

approaches: (i) the crystal structure unequivocally shows that absence of SAM does not affect the overall conformation of DENV MTase, including the SAM-binding pocket; (ii) depletion of SAM from the recombinant MTase did not change the activities of cap methylations and GMP-MTase complex formation. These results, together with the established protocol for preparation of SAM-depleted MTase, have made it possible to search for compounds that can bind to the SAM-binding pocket and compete against SAM binding. A number of biophysical assays, such as surface-plasmon resonance or differential-scanning fluorimetry, can be envisioned. One potential challenge of this approach is the requirement of inhibitors with high affinity for the SAM-binding pocket in order to efficiently compete against the authentic ligand SAM. In line with this idea, SAH analogs that interact with a flavivirus MTase-specific pocket (located adjacent to the SAM-binding pocket) were reported to selectively inhibit DENV MTase without suppression of cellular MTases (Lim et al., 2011). Since flavivirus MTase is a genetically-validated antiviral target (Zhou et al., 2007), the proposed approach warrants further studies for flavivirus antiviral development.

Acknowledgements

We thank colleagues at Novartis Institute for Tropical Diseases for helpful discussions during the course of this study and the beamline scientists at the Swiss Light Source for assistance with data collection.

References

Assenberg, R., Ren, J., Verma, A., Walter, T.S., Alderton, David., Hurrelbrink, R.J., Fuller, S.D., Bressanelli, S., Owens, R.J., Stuart, D.I., Grimes, J.M., 2007. Crystal structure of the Murray Valley encephalitis virus NS5 methyltransferase domain in complex with cap analogues. J. Gen. Virol. 88, 2228–2236.

Bollati, M., Milani, M., Mastrangelo, E., Ricagno, S., Tedeschi, G., Nonnis, S., Decroly, E., Selisko, B., de Lamballerie, X., Coutard, B., Canard, B., Bolognesi, M., 2009. Recognition of RNA cap in the Wesselsbron virus NS5 methyltransferase domain: implications for RNA-capping mechanisms in Flavivirus. J. Mol. Biol. 385, 140–152.

Decroly, E., Ferron, F., Lescar, J., Canard, B., 2012. Conventional and unconventional mechanisms for capping viral mRNA. Nat. Rev. Microbiol. 10, 51–65.

Dong, H., Chang, D.C., Hua, M.H., Lim, S.P., Chionh, Y.H., Hia, F., Lee, Y.H., Kukkaro, P., Lok, S.M., Dedon, P.C., Shi, P.Y., 2012. 2′-*O* methylation of internal adenosine by flavivirus NS5 methyltransferase. PLoS Pathog. 8, e1002642.

Dong, H., Chang, D.C., Xie, X., Toh, Y.X., Chung, K.Y., Zou, G., Lescar, J., Lim, S.P., Shi, P.Y., 2010. Biochemical and genetic characterization of dengue virus methyltransferase. Virology 405, 568–578.

Dong, H., Fink, K., Zust, R., Lim, S.P., Qin, C.F., Shi, P.Y., 2014. Flavivirus RNA methylation. J. Gen. Virol. 95, 763–778.

Egloff, M.P., Benarroch, D., Selisko, B., Romette, J.L., Canard, B., 2002. An RNA cap (nucleoside-2′-*O*-)-methyltransferase in the flavivirus RNA polymerase NS5: crystal structure and functional characterization. EMBO J. 21, 2757–2768.

Egloff, M.P., Decroly, E., Malet, H., Selisko, B., Benarroch, D., Ferron, F., Canard, B., 2007. Structural and functional analysis of methylation and 5′-RNA sequence requirements of short capped RNAs by the methyltransferase domain of dengue virus NS5. J. Mol. Biol. 372, 723–736.

Fink, K., Shi, P.Y., 2014. Live attenuated vaccine: the first clinically approved dengue vaccine? Exp. Rev. Vaccines 13, 185–188.

Geiss, B.J., Thompson, A.A., Andrews, A.J., Sons, R.L., Gari, H.H., Keenan, S.M., Peersen, O.B., 2009. Analysis of flavivirus NS5 methyltransferase cap binding. J. Mol. Biol. 385, 1643–1654.

Ghosh, A., Lima, C.D., 2010. Enzymology of RNA cap synthesis. Wiley Interdiscip. Rev. RNA 1, 152–172.

Hodel, A.E., Gershon, P.D., Shi, X., Quiocho, F.A., 1996. The 1.85 A structure of vaccinia protein VP39: a bifunctional enzyme that participates in the modification of both mRNA ends. Cell 85, 247–256.

Issur, M., Geiss, B.J., Bougie, I., Picard-Jean, F., Despins, S., Mayette, J., Hobdey, S.E., Bisaillon, M., 2009. The flavivirus NS5 protein is a true RNA guanylyltransferase that catalyzes a two-step reaction to form the RNA cap structure. RNA 15, 2340–2350.

Jansson, A.M., Jakobsson, E., Johansson, P., Lantez, V., Coutard, B., de Lamballerie, X., Unge, T., Jones, T.A., 2009. Structure of the methyltransferase domain from the Modoc virus, a flavivirus with no known vector. Acta Crystallogr. D Biol. Crystallogr. 65, 796–803.

Li, S.H., Dong, H., Li, X.F., Xie, X., Zhao, H., Deng, Y.Q., Wang, X.Y., Ye, Q., Zhu, S.Y., Wang, H.J., Zhang, B., Leng, Q.B., Zuest, R., Qin, E.D., Qin, C.F., Shi, P.Y., 2013. Rational design of a flavivirus vaccine by abolishing viral RNA 2′-*O* methylation. J. Virol. 87, 5812–5819.

Lim, S.P., Sonntag, L.S., Noble, C., Nilar, S.H., Ng, R.H., Zou, G., Monaghan, P., Chung, K.Y., Dong, H., Liu, B., Bodenreider, C., Lee, G., Ding, M., Chan, W.L., Wang, G., Jian, Y.L., Chao, A.T., Lescar, J., Yin, Z., Vedananda, T.R., Keller, T.H., Shi, P.Y., 2011. Small molecule inhibitors that selectively block dengue virus methyltransferase. J. Biol. Chem. 286, 6233–6240.

Lim, S.P., Wang, Q.Y., Noble, C.G., Chen, Y.L., Dong, H., Zou, B., Yokokawa, F., Nilar, S., Smith, P., Beer, D., Lescar, J., Shi, P.Y., 2013. Ten years of dengue drug discovery: progress and prospects. Antiviral Res. 100, 500–519.

Mastrangelo, E., Bollati, M., Milani, M., Selisko, B., Peyrane, F., Canard, B., Grard, G., de Lamballerie, X., Bolognesi, M., 2007. Structural bases for substrate recognition and activity in Meaban virus nucleoside-2′-*O*-methyltransferase. Protein Sci. 16, 1133–1145.

Menachery, V.D., Yount Jr., B.L., Josset, L., Gralinski, L.E., Scobey, T., Agnihothram, S., Katze, M.G., Baric, R.S., 2014. Attenuation and restoration of severe acute respiratory syndrome coronavirus mutant lacking 2′-*O*-methyltransferase activity. J. Virol. 88, 4251–4264.

Noble, C.G., Beuth, B., Taylor, I.A., 2007. Structure of a nucleotide-bound Clp1-Pcf11 polyadenylation factor. Nucleic Acids Res. 35, 87–99.

Noble, C.G., Shi, P.Y., 2012. Structural biology of dengue virus enzymes: towards rational design of therapeutics. Antiviral Res. 96, 115–126.

Ray, D., Shah, A., Tilgner, M., Guo, Y., Zhao, Y., Dong, H., Deas, T., Zhou, Y., Li, H., Shi, P.-Y., 2006. West nile virus 5′-cap structure is formed by sequential guanine N-7 and ribose 2′-*O* methylations by nonstructural protein 5. J. Virol. 80, 8362–8370.

Shuman, S., Hurwitz, J., 1981. Mechanism of mRNA capping by vaccinia virus guanylyltransferase: characterization of an enzyme–guanylate intermediate. Proc Natl. Acad. Sci. U.S.A. 78, 187–191.

Zhou, Y., Ray, D., Zhao, Y., Dong, H., Ren, S., Li, Z., Guo, Y., Bernard, K., Shi, P.-Y., Li, H., 2007. Structure and function of flavivirus NS5 methyltransferase. J. Virol. 81, 3891–3903.

Zust, R., Dong, H., Li, X.F., Chang, D.C., Zhang, B., Balakrishnan, T., Toh, Y.X., Jiang, T., Li, S.H., Deng, Y.Q., Ellis, B.R., Ellis, E.M., Poidinger, M., Zolezzi, F., Qin, C.F., Shi, P.Y., Fink, K., 2013. Rational design of a live attenuated dengue vaccine: 2′-*O*-methyltransferase mutants are highly attenuated and immunogenic in mice and macaques. PLoS Pathog. 9, e1003521.